Journal of Applied Fluid Mechanics, Vol. 11, No. 1, pp. 55-63, 2018.
Available online at www.jafmonline.net, ISSN 1735-3572, EISSN 1735-3645.
DOI: 10.29252/jafm.11.01.27906

Hydrodynamics in Two-Phase Turbulent Boundary Layers

M. Dhahri[1†] and H. Aouinet[2]

[1]*University of Sousse, Higher Institute of Agricultural Sciences of Chott Mariem, BP N° 47, 4042 Sousse, Tunisia*
[2]*University of Tunis El Manar, National Engineering School of Tunis BP N°37, Le Belvedere, 1002 Tunis, Tunisia*

†*Corresponding Author Email: maher.dhahri@enit.utm.tn*

(Received April 22, 2017; accepted September 12, 2017)

ABSTRACT

The corrections for log law must be taken into account the presence of bubbles in the two phase turbulent boundary layer. In the present study, a logarithmic law for the wall based on the supposition of additional turbulent viscosity associated with bubble wakes in the boundary layer was proposed for bubbly flows. An empirical constant accounting both for shear induced turbulence interaction and for non-linearity of bubble was determined for the new wall law, this constant was deduced from experimental measurements. In the case of a turbulent boundary layer with millimetric bubbles developing on a vertical flat plate, the wall friction prediction achieved with the wall law was compared to the experiences. We obtained a good concordance between experimental and numerical result. This significant agreement for wall friction prediction was particularly important for the low void fraction when bubble induced turbulence have a considerable role.

Keywords: Bubbly two phase flows; Wall law; Turbulent boundary layer.

NOMENCLATURE

B	two-phase correction in two-phase wall law
$C_{\varepsilon 2}$	single phase turbulence constant
C_D	drag force coefficient
C_L	lift force coefficient
C_{TD}	turbulent dispersion force coefficient
C_{vm}	virtual mass force coefficient
C_W	wall lubrication force coefficient
C_{w1}	first wall lubrication force
C_{w2}	second wall lubrication force coefficient
$C\mu$	single-phase turbulence constant
$C_{\varepsilon 1}$	single-phase turbulence constant
K	von karman constant
K_l	non-linearity factor in two-phase wall law
v	turbulent viscosity
SP	refers to single-phase
TP	refers to two-phase
Ur	slip velocity
Uw	frictional velocity
v	velocity
x	coordinate
Y_0^+	non-dimensional viscous sublayer thickness
α	void fraction
ρ	density
σ	instant general stress tensor
τ	instant shear stress tensor
$+$	wall normalized value

1. INTRODUCTION

In a wide variety of engineering systems, the turbulent bubbly two phase flows play an essential role in many domains such as heat exchangers, petroleum transportation systems and nuclear reactors. Therein, accurate predictions of the flow characteristics are essentially required for the design, process optimization and safety control. With the development of the experimental techniques and computational fluid dynamics (CFD), numerous researches on the turbulent bubbly flow have been carried out (Lopez de Bertodano *et al*. (1994), Frank *et al*. (2008), Dhahri *et al*. (2013), etc. on the basis of the improvement of understanding and modeling the turbulent bubbly flow. Nevertheless, the presence of the multi-deformable and moving interfaces therein could make considerable discontinuities of the complex flow properties near the interface. To understand the physical process and develop the model of the turbulent bubbly flows, the detailed flow

Table 1 Summary of proposed near –wall function for two phase flow simulation

Parameter	Marie (1997)	Troshko (2001)	Mikielewics(2003)	Ramstorfer (2008)
General form	$U^+ = \frac{1}{\kappa^x}\ln y^+ + B^x$	$U^+ = \frac{1}{\kappa^x}\ln y^+ + B^x$	$U^+ = \frac{1}{\kappa^x}\ln(\kappa^x / y^+) + B^x$	$U^+ = \frac{1}{\kappa^x}\ln(y^+) + B^x - \Delta U^+$
Correction factor	$\beta = \left[1-(g\frac{d}{U_*^2})(\varepsilon_p - \varepsilon_E\right]^{0.5}$	$\beta = \left[(1+\frac{\alpha_{\max}U_r}{\kappa U_*})(1-\alpha_{\max})\right]^{-1}$	$\beta = (1-\alpha)^{0.5}$	$\beta = \left[-2\log(\frac{2.51}{R_e\sqrt{\beta}}+0.27C_{kre})\right]^{-2}$
Additive constant	$B^x = B + y_+^0(\frac{1}{\beta}-1) - \frac{1}{\kappa}\ln(\beta)$	$B^x = y_+^0(1-\beta) + \beta B$	$B^x = 7.7$	$B^x = B$
Von karmen constant	$\kappa^x = \beta^{-1}\kappa$	$\kappa^x = \beta^{-1}\kappa$	$\kappa^x = \beta\kappa$	$\kappa^x = \kappa$
End of viscous layer	$y_+^0 = 11$	$y_+^0 = 11$	$y_+^0 = 8$	$y_+^0 = 11$

information such as the drag resistance, the temporal and spatial evolutions of velocities and turbulence in two phases and the detailed characteristic of bubbles such as the bubble concentration, the bubble size, the bubble shape and the bubble motion are necessary.

In the case of boundary layer flow multiple efforts for the modeling and understanding of the flow characteristics and physical process have been performed. The experimental data in two-phase bubbly flows developed on a vertical flat plate show that the velocity profiles has a logarithmic behavior near the wall and indicate that the constants of the logarithmic profiles are sensibly modified and depend on the amplitude of the wall void fraction peaking by the use of the k-□ model for the closure of Reynolds stress in the continuous phase. Over the last few years, there have been serious efforts to understand the near-wall region of gas-liquid, bubbly turbulent flows and to propose wall-functions specifically designed for these flows (Guan *et al*. (2015), Santarelli *et al*. (2016)).

Moursali *et al*. (1995) developed and focused their measurements on the distribution of the mean liquid velocity, the wall shear stress and the void faction in an upward turbulent bubbly boundary layer with the LDV technique. According to their study, the lateral bubble migration toward to the wall occurs depending on the bubble mean diameter and the void fraction similar to the duct flow. In addition, the wall skin friction coefficient was observed to increase because of the presence of the bubbles, which modifies the universal logarithmic law near the wall. This supports the experience of Marie *et al*. (1997) on a vertical flat plate. The authors showed that the slope of the logarithmic law tends to decrease when the peak of void fraction is located in the logarithmic region. Based on the asymptotic methodology, Mikielewicz (2003) proposed a near wall function and they developed two approaches: The first based on the effect of an assumed constant on the void fraction distribution, the second based on the prediction of the wall peaking effect. Mikielewicz (2003) compared his advances with the measurements of Marie *et al*. (1997). Hideki Murakawa *et al*. (2003) performed experiment of a turbulent boundary layer for bubbly flow in a 20mm×100mm vertical rectangular channel. The authors obtained the acceleration of the liquid velocity in the vicinity of the wall when liquid flow rate is reduced. Recently, Yassin A *et al*. (2014) used an innovative measuring techniques PTV (Particle Tracking Velocimetry). Measurements of the liquid parameters such as the velocity, RMS of the liquid velocity, and Reynolds stress were provided. More recently, Avinash *et al*. (2016) proposed a new two-fluid model averaging near the wall; this advance is tested with the boundary layer experience, laminar flow and turbulent flow in pipes. Best agreements between the numerical results with the experimental data are obtained by the models based on a single-phase logarithmic wall law without the validation of this law for turbulent bubbly boundary layer.

Table 1 summarizes some proposed models based on a logarithmic assumption to develop a near wall function taking into consideration the good prediction for the single phase turbulent flows. Different constant and empirical correlations are obtained. This lack of detailed information is the purpose of the motivation of this present work. The idea of this paper is to obtain a direct formulation of two-phase logarithmic wall law. The presented wall law contained empirical constant which was deduced from experimental data. In this first part, we presented the wall law for two-phase turbulent boundary layers. Finally we compare our results to the measurements of a turbulent boundary layer obtained by Marie *et al*. (1997) developing on a vertical flat plate with millimetric bubbles.

2. TWO-FLUID MODEL FOR TURBULENT BUBBLY FLOWS

2.1 Mass and Momentum Equations

The CFD calculations were performed with the numerical ANSYS CFX 15.0 code. In the case of stationary and incompressible two phase flows, the mass and momentum equations without mass transfer are expressed in this code for each phase k as:

$$\frac{\partial}{\partial t}(\rho_k\alpha_k) + \frac{\partial}{\partial x_i}(\alpha_k\rho_k\overline{\overline{u_{ki}}}) = m_k \tag{1}$$

$$\frac{\partial}{\partial t}\left[\alpha_k\rho_k\overline{\overline{u_k}}\right] + \frac{\partial}{\partial x_j}\left[\alpha_k\rho_k\overline{\overline{u_{ki}u_{kj}}}\right] = -\alpha_k\frac{\partial\overline{\overline{p_k}}}{\partial x_i} + \frac{\partial}{\partial x_j}\alpha_k\left[\overline{\overline{\tau_{kj}}} + \overline{\overline{\tau_{kj}^t}}\right] + \alpha_k\rho_k g_i + M_{ki} + \sum_j \overline{\overline{m_{k,j}u_j}} \tag{2}$$

Where m_k is the interfacial mass source and M_{ki} is the interfacial momentum exchange on phase k. In the equation, the average stress tensor is written as:

$$\overline{\overline{\sigma_{k,ij}}} = -p_k \overline{\overline{\delta_{ij}}} + \overline{\overline{\tau_{kj}}} \tag{3}$$

$\overline{\overline{\tau_{kj}^t}}$ Represent the turbulent stress tensor, it's defined as:

$$\overline{\overline{\tau_{kj}^t}} = \rho_k \overline{\overline{u_{kj}' u_{kj}'}} \tag{4}$$

2.2 The Momentum Interfacial Transfer in CFD Model

The momentum interfacial transfer includes the contributions of the average forces (drag, turbulent diffusion, lift and added mass forces):

$$\begin{aligned} < M_{ki} > &= < M_{ki}^{D} > + < M_{ki}^{L} > \\ &+ < M_{ki}^{VM} > + < M_{ki}^{TD} > \end{aligned} \tag{5}$$

Drag Force

The drag force obtained from the classical theory is:

$$\begin{aligned} < M_{Li}^{D} > &= - < M_{Gi}^{D} > \\ &= \frac{3}{4} \frac{C_D}{d} \alpha \rho_L \left| \overline{\overline{u_{Ri}}} \right| \overline{\overline{u_{Ri}}} \end{aligned} \tag{6}$$

Where d is the bubble diameter and C_D is the drag coefficient of the bubbles. Different correlations for the drag coefficient are implemented in CFX code (Shiller and Naumaan (1933), Ishii and Zuber (1979)).

Lift Force

The lift force is given by:

$$\begin{aligned} < M_{Li}^{L} > &= - < M_{Gi}^{L} > \\ &= \rho \alpha C_L \left(\frac{\partial \overline{\overline{u_j}}}{\partial x_i} - \frac{\partial \overline{\overline{u_i}}}{\partial x_j} \right) \left(\overline{\overline{u_{Gi}}} - \overline{\overline{u_{Li}}} \right) \end{aligned} \tag{7}$$

The lift coefficient value used in CFX code is calculated by different correlations (Saffman Mei *et al.* (1968), Legendre and Magnaudet (1998) and Tomiyama *et al.* (1998))

Mass Force

The virtual mass force is expressed as Troshko and Hassen (2001):

$$M_C^{Vm} = \alpha_G \rho_L C_{vm} \left(\frac{D_G U_G}{Dt} - \frac{D_L U_L}{Dt} \right) \tag{8}$$

Where C_{vm} is the virtual mass coefficient that depend on the void fraction. Many authors have used constant values for C_{vm}. As an example, Drew and Lahey (1982) used 0.5, Kuo and Wallis (1988) proposed values within the range 2.0 ~ 3.0, Lance and Bataille (1991) suggested values between 1.2 and 3.4. Lopez de Bertodano (1994) suggested the value of 1.2 for the high void fraction case and the value of 2 for the ellipsoidal bubbles.

The interfacial pressure difference Lamb (1932) is:

$$\left(p_i - P_C \right) = -C_p \rho_L \left| U_R \right|^2 \alpha_L \tag{9}$$

Drew and Lahey (1982) recommended Cp =1.0. The constant of Schiller and Naumann (1933) was used in there model Cp =0.

Turbulent Dispersion Force

The turbulent dispersion force is calculated by CFX code with two formulations which the dispersion effect is proportional to void fraction gradients: the Favre (2006) and the Lopez de Bertodano (1994) models respectively written as:

$$\begin{aligned} < M_{Li}^{TD} > &= - < M_{Gi}^{TD} > \\ &= C_{TD} C_{cd} \frac{\nu_t}{\sigma_t} \left(\frac{\partial \alpha}{\alpha \partial x_i} - \frac{\partial (1-\alpha)}{(1-\alpha) \partial x_i} \right) \end{aligned} \tag{10}$$

$$\begin{aligned} < M_{Li}^{TD} > &= - < M_{Gi}^{TD} > \\ &= - \frac{C_{TD}}{\alpha} \rho_L k_L \frac{\partial \alpha}{\partial x_i} \end{aligned} \tag{11}$$

Where k_L is the liquid turbulent energy and C_{TD} is a turbulent dispersion coefficient that take a value between 0 and 1.

Wall Force

The wall force formulation proposed by Antal *et al.* (1991) is implemented in CFX code. This force represents the effect that keeps the centers of the bubbles no closer than approximately one bubble radius from the wall and it given as:

$$< M_{Li}^{W} > = \alpha \rho_L C_W \left| u_R \right|^2 n_w \tag{12}$$

$$C_w = \min \left(0; -\left(\frac{C_1^W}{d_B} + \frac{C_2^W}{y_{wall}} \right) \right) \tag{13}$$

Where n_w is the normal inward vector and y_{wall} is the distance from the wall. The values of the coefficients appeared in the equations are defined in CFX code by:

$$C_1^w = -0.01 \ , \ C_2^w = 0.05 \ .$$

2.3 Turbulence Modeling

The formulation for the momentum turbulent diffusivity of the continuous phase in CFX code is given by Sato *et al.* (1981) where the authors proposed the sum of the shear-induced and bubble-induced turbulent viscosities:

$$\nu_t = \nu_{t,SI} + \nu_{t,BI} \tag{14}$$

Where the first term corresponds to the k-ε model for the shear induced diffusivity and the second term corresponds to Sato *et al.*'s (1981) model for the bubble induced diffusivity that written

respectively as:

$$\nu_{t,SI} = c_\mu \rho \frac{k_L^2}{\varepsilon} \tag{15}$$

$$\nu_{t,BI} = 0.6 \rho_L \alpha d \left| \overline{\overline{u_R}} \right| \tag{16}$$

The coefficient $C_\mu = 0.09$ is the standard value for the k-ε model. In case of a standard k-ε model implemented in CFX code, two additional balance equations have to solve. The turbulent kinetic energy of the liquid phase is written as:

$$\frac{\partial}{\partial t}((1-\alpha)\rho_L k_L) + \frac{\partial}{\partial x_j}((1-\alpha)(\rho_L \overline{\overline{u_{Li}}} k_L - (\nu + \frac{\nu_{t,SI}}{\sigma_k})\frac{\partial}{\partial x_j} k_L)) = \alpha(P_L - \rho_L \varepsilon_L) + S^k \tag{17}$$

And the conservation equation for the dissipation rate is written as:

$$\frac{\partial}{\partial t}((1-\alpha)\rho_L \varepsilon_L) + \frac{\partial}{\partial x_j}((1-\alpha)(\rho_L \overline{\overline{u_{Li}}} \varepsilon_L - (\nu + \frac{\nu_{t,SI}}{\sigma_\varepsilon})\frac{\partial}{\partial x_j} \varepsilon_L)) = \alpha \frac{\varepsilon_L}{k_L}(C_{\varepsilon 1} P_L - C_{\varepsilon 2} \rho_L \varepsilon_L) + S^\varepsilon \tag{18}$$

Here ν is the molecular viscosity; $\nu_{t,SI}$ is the shear induced turbulent viscosity; S^k, S^ε are source terms due to presence bubbles and P_L is the turbulence production rate:

$$P_L = -\overline{\overline{u'_{Li} u'_{Lj}}} \frac{\partial \overline{\overline{u_{Li}}}}{\partial x_j} = 2\nu_t \frac{\partial \overline{\overline{u_{Li}}}}{\partial x_j} S_{ij} \tag{19}$$

$$S_{ij} = \frac{1}{2}\left(\frac{\partial \overline{\overline{u_{Li}}}}{\partial x_j} + \frac{\partial \overline{\overline{u_{Lj}}}}{\partial x_i}\right) \tag{20}$$

Constants $C_{\varepsilon 1} = 1.44, C_{\varepsilon 2} = 1.92, \sigma_k = 1, \sigma_\varepsilon = 1.3$ are defined in the standard single-phase flow k-ε model.

3. TWO PHASE WALL LAW

In this section, we use the experimental results obtained by Marie *et al.* (1997) for the turbulent boundary layer case on a vertical flat plate with millimetric bubbles. The logarithmic plot of the velocity in terms of the inner variable, $y^+ = \frac{u_* y}{\nu}$, shows that the presence of three zones usually encountered in a single-phase boundary layer (viscous sublayer, logarithmic zone, and the wake region) are preserved (Fig. 1).

In the logarithmic zone, $30 \le y+ \le 200$, the experimental data of Marie *et al.* (1997) shows that the velocity distribution can be described by a logarithmic law whose constants κ and C differ from the single-phase flow values, κ^{SP} and C^{SP} and functions of the peak void fraction and the mean liquid velocity. By attaching the turbulent friction in two-phase flow to the one in the single-phase flow, we will determine the constants κ^{TP} and C^{TP} of the logarithmic law in two-phase flow:

$$\frac{\overline{U}}{U_w^{TP}} = \frac{1}{\kappa^{TP}} \ln(y_+) + C^{TP} \tag{21}$$

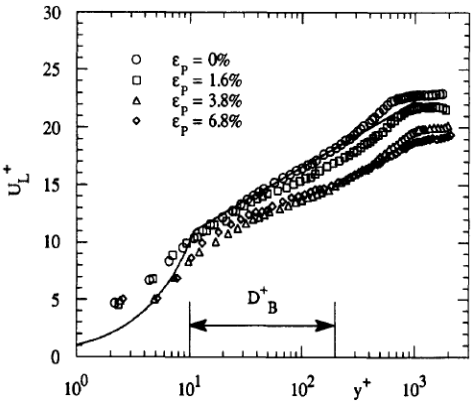

Fig. 1. Velocity profile plotted in inner variables. (Marie *et al.* (1997)).

In single-phase flow, the logarithmic law is given by:

$$\frac{\overline{U}}{U_w^{SP}} = \frac{1}{\kappa^{SP}} \ln(y_+) + C^{SP} \tag{22}$$

Where

$$\frac{\overline{U}}{U_w^{TP}} \tag{23}$$

is the normalized liquid velocity parallel to the wall

$$y_+ = \frac{y U_w^{TP}}{\nu_C} \tag{24}$$

is the normalized distance normal to the wall

$$U_w^{TP} \tag{25}$$

is the two-phase frictional velocity defined as,

$$U_w^{TP} = \sqrt{\frac{\tau_w^{TP}}{\rho}} \tag{26}$$

τ_w^{TP} is the two-phase wall shear stress applied on continuous phase.

Let us consider a two-dimensional, developed, incompressible two phase turbulent boundary layer with y is the distance from the wall, the x component of the continuous phase momentum equation can be written as Troshko (2000):

$$\frac{\partial[\rho_l \alpha_l U_l U_l]}{\partial x} + \frac{\partial[\rho_l \alpha_l U_l V_l]}{\partial y} = -\alpha \frac{\partial P}{\partial x} + M_{lx}^d + \rho_l \alpha_l g_x + \frac{\partial}{\partial x}\left(\alpha_l \left(2\nu_l \frac{\partial U_l}{\partial x} - \langle \tau_{lxx} \rangle^{Re}\right)\right)$$

$$+\frac{\partial}{\partial y}\left(\alpha_l\left(\nu_l(\frac{\partial U_l}{\partial y}+\frac{\partial V_l}{\partial y})-\langle\tau_{lxx}\rangle^{\mathrm{Re}}\right)\right) \tag{27}$$

Where U_c and V_c are the wall tangential and normal components of the mean liquid velocity.

In the inner layer the turbulence is predominant so that the interfacial force density is neglected .it is assumed that in the coquette assumption of the single phase the variation of all dependent variables in the longitudinal direction are neglected with these assumptions equations 1 reduces to:

$$\frac{\partial}{\partial y}\left(\alpha_l\left(\nu_l\frac{\partial U_C}{\partial y}+\langle\tau_{lxy}\rangle^{\mathrm{Re}}\right)\right) \tag{28}$$

Using the eddy viscosity model, the Reynolds stress equation can be obtained as:

$$\langle\tau_{lxy}\rangle^{\mathrm{Re}}=\nu_l^t\frac{\partial U_l}{\partial y} \tag{29}$$

Integrating the Eq. (28) and taking into account Eq. (29) the equation that describes boundary layer is as follows:

$$\tau_w^{TP}=\rho_l\left(\nu_l+\nu_l^t\right)\frac{\partial U_l}{\partial y} \tag{30}$$

Holds the log layer is dominated by the turbulence effects, Eq. 4 reduces to:

$$\left(U_w^{TP}\right)^2=\alpha_l\nu_l^t\frac{\partial U_l}{\partial y} \tag{31}$$

In the log region it is assumed that the liquid turbulent stress can be represented as the sum of two components. The first component accounts for shear induced turbulence. The second component is associated with the wakes of bubbles present in the inner layer. Holds under the condition that Boussinesq hypothesis is valid for the following components, we shall write the total turbulent viscosity as Troshko (2000):

$$\nu_l^t=\nu_l^{out}+\nu_l^{in} \tag{32}$$

Where ν_l^{out} and ν_l^{in} is associated with the first and second stress components, respectively. The conventional shear induced turbulent viscosity defined by (Wilcox, 1993):

$$\nu_l^{out}=\kappa^{SP}yU_w^{TP} \tag{33}$$

To determine the induced turbulent viscosity, we suggest that it is the product of the void-fraction peak near the wall α_p, the slip velocity, a large flat profile portion at the constant value α_E and the distance from the wall y. This assumption is supported by the experimental data. Thus, we have proposed the following formulation for ν_l^{in} :

$$\nu_C^{in}=\kappa_l y\left(\alpha_p-\alpha_E\right)U_r \tag{34}$$

U_r is the local slip velocity and κ_l is an empirical correction factor. This correction is introduced to take into consideration the non-linear interaction between bubbles and shear induced turbulence fields.

Substitution of Eqs. (33) and (34) into Eq. (32) and subsequently into Eq. (30), we can derive the velocity gradient for low void fraction in a two-phase boundary layer:

$$\frac{dy}{\kappa^{SP}y}=\frac{dU_C}{\chi U_w^{TP}} \tag{35}$$

Where

$$\chi=\left[\left(1-\alpha_g\right)\left[1+\frac{\alpha_p U_r K_L}{\kappa^{SP}U_w^{TP}}-\frac{\alpha_E U_r K_L}{\kappa^{SP}U_w^{TP}}\right]\right]^{-1} \tag{36}$$

is the correction coefficient.

A new frictional velocity is introduced

$$U_w^{(TP)c}=\chi U_w^{TP} \tag{37}$$

Then, a solution of (27) will be the logarithmic law:

$$U_+^{(TP)c}=\frac{1}{\kappa^{TP}}\ln\left(y_+^c\right)+C^{(TP)c} \tag{38}$$

Where all wall variables are calculated using new velocity scale:

$$U_+^{(TP)c}=\chi U_+^{TP} \tag{39}$$

$$\kappa^{TP}=\kappa^{SP}\chi^{-1} \tag{40}$$

Local slip velocity in (36) was evaluated using the distorted bubble expression (41):

$$U_r=0.934\left(1+1.41\alpha\right)j+1.53\left(\frac{\sigma g}{\rho_L}\right)^{1/4} \tag{41}$$

Where σ: the surface tension, g: gravitational acceleration, J: superficial velocity, ρ: Density of liquid.

K_L can be approximated after extensive computer tests by:

$$\kappa_L=0.0021\ \ln\left(1.497\,U_W^{TP}\right) \tag{42}$$

On the other hand and in spite of some spread data, Moursali *et al.* (1995) showed that the non-dimensional thickness of the viscous sublayer that it can determined in the velocity profile as the ordinate of the intersection of the linear and logarithmic parts is almost constant. So, we can determine the constant $C^{(TP)c}$ as:

$$C^{(TP)C}=10\left(1-\chi^{-1}\right)+4.9\chi \tag{43}$$

4. RESULTS AND DISCUSSIONS

4.1 CFD Simulation Set-Up

In the present study, we performed the geometry configuration of Moursali *et al*. (1995). The measurements developed in a vertical turbulent bubbly boundary layer based on LDV technique. The experimental data are obtained at typical conditions with atmospheric pressure, ambient temperature and at liquid velocities less than 1.5 m/s in a 2.5 m square channel with a 50 m^3tap water tank, Fig.2. The cross section is 400 × 400 mm^2 where the gas is injected uniformly into the liquid. Therein; the authors interested on the void fraction data, the wall shear stress, and the mean liquid velocity measurements.

According to their study, the lateral bubble migration toward to the wall occurs depending on the bubble mean diameter and the void fraction similar to the duct flow.

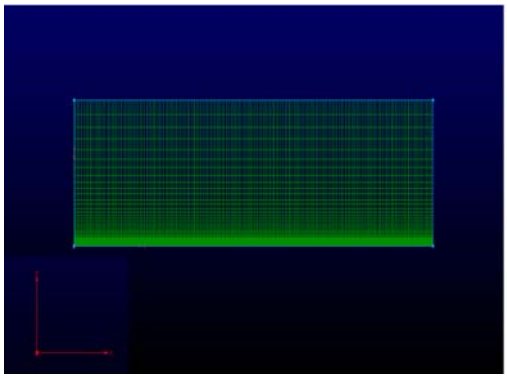

Fig. 2. The Computational Domain and Typical CFX Mesh.

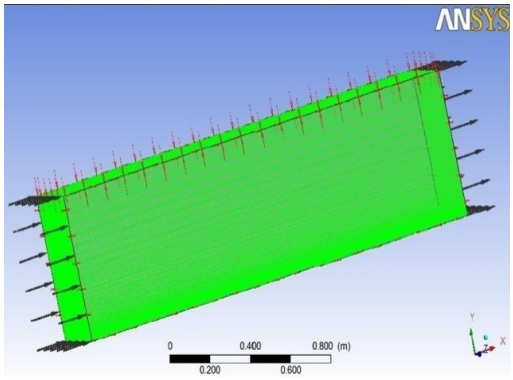

Fig. 3. Computational Domain.

The computations were performed using (CFX 15.0). In this work, the drag force and the lift force proposed respectively by Ishii and Zuber (1979) and Tomiyama (1998) are used. The Lopez de Bertodano *et al*. (1994) formulation for the turbulent dispersion force, the wall force by Antal *et al*. (1991) and the Sato *et al*. (1981) eddy viscosity are also obtained. Geometric modeling and meshing was made by the Pointwise 16.0 software. Convergence was tested by requiring the sum of the absolute residual values to be less than 10^{-6}. The residual value is calculated for each solved variable and it is equal to the absolute difference between left- and right-hand sides of the different equations are solved at each node point. The final mesh is shown in Fig. 2.

4.2 Single-Phase Boundary Layer

In this part, the computational results are compared with experimental data of Moursali *et al*. (1995) obtained for an air-water flow in a vertical channel. Figs.4, 5 represent respectively the liquid velocity, the logarithmic profile of velocity. Fig. 4 shows that the velocity profile was well predicted by the model. The profile of experimental velocity represents a boundary layer located at section x=22 mm from the wall; this result has been found by the numerical simulation in Fig. 5. The agreement between our model and data is shown by comparison with data of the single-phase wall-bounded flow theory where the presence of three classical zones is conserved: Viscous sublayer, logarithmic zone, and the wake region. The concordance is quite good except near the wall.

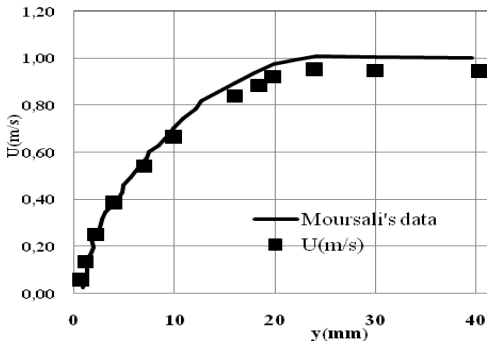

Fig. 4. Comparison of the liquid velocity profile with experimental results single phase flow.

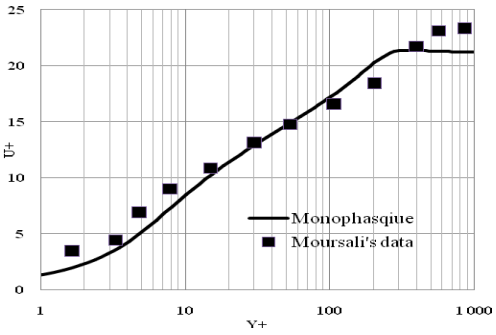

Fig. 5. Mean velocity predictions: Comparison with experimental results.

4.3 Two Phase Boundary Layer

The applications of the wall law postulated in wall bounded bubbly flows confirm the importance of the significant developments proposed to ameliorate the predetermination of the turbulence structure. Figs. 6-8 show a satisfactory concordance accord between the simulated results and the experimental points of Marie *et al.* (1997): our results have led to

the adjustment for the constant K_L.

This result is confirmed by the good concordance with all near-wall experimental measurements for y+ ranging between 40 and 1000 for the two low void fractions (0.2% and 0.5%). Remember that these experiences indicate a logarithmic behaviour of velocity profiles in bubbly flows near the wall; however the logarithmic law applies to these profiles with constants different from those of the case of single-phase boundary layer.

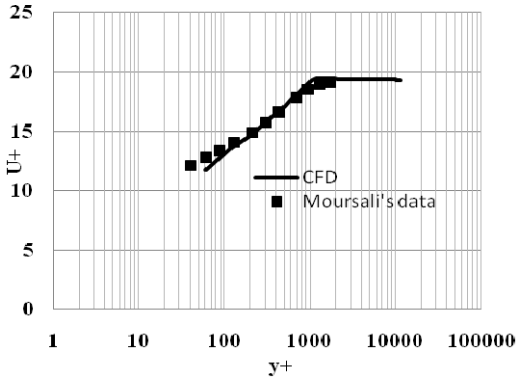

Fig. 6. Velocity profile plotted using the model (UL=1m/s; void fraction=0.5%): Comparison with experimental results.

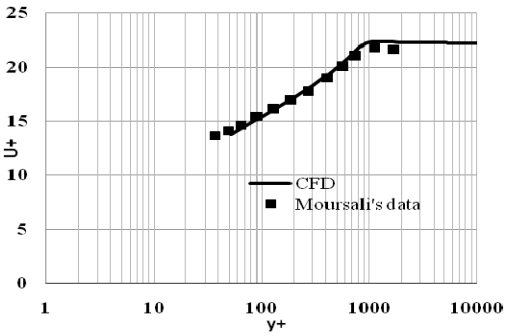

Fig. 7. Velocity profile plotted using the model (UL=1m/s; void fraction=0.2%): Comparison with experimental results.

For the higher void fraction case (1.5%) as can be seen from Fig. 8, in the range y+ = 40-200, the increase of the wall function curve is steeper than the inclination of experimental data. This designates that we should improve more the proposed model. This lack may be explained by one of the missing effects like the influence of detached bubbles on turbulent mixing in bubbles boundary layer and the buoyancy effect. However, the present model shows important perfection over the single-phase wall law and is establish to be correct the calculation of velocity in the first near wall cell of numerical domain.

In this work we study also the void fraction profile in the vertical bubbly boundary layer in comparison with Moursali *et al*. (1995) experimental data. The Fig. 9 shows clearly that the two-fluid model with the wall law proposed succeeds to reproduce the near wall void fraction distribution. We can observed in the void fraction distribution a maximum sharp at the wall, α_p, and a large flat part at the constant value, α_e=0, 01. The same figure shows also that the peaking void fraction α_p is located at a distance from the wall of the order of mean equivalent radius of the bubbles.

On the other hand, consider that the quality of the determination of the void fraction profiles is directly related to the excellence of the prediction of the fluctuating flow fields in bubbly flow in an opposite manner. For that reason, we plotted the Fig. 10 that present the numerical turbulent intensity distribution in two boundary layer flows for the void fraction (α=0.015) in comparison with the experience of Moursali *et al*. (1995).

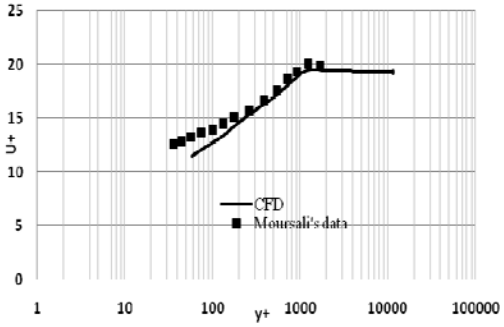

Fig. 8. Velocity profile plotted using the model (UL=1m/s; void fraction=1.5%): Comparison with experimental results.

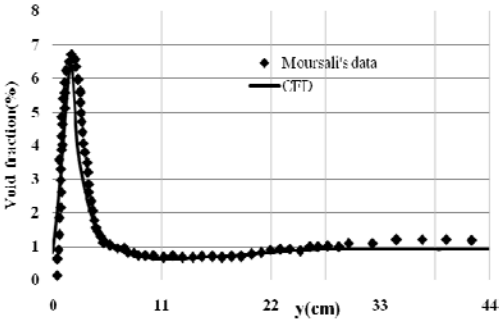

Fig. 9. Void fraction profile in vertical bubbly boundary layer: Comparison with the experimental data of Moursali *et al.* (1995) - (void fraction=0, 01).

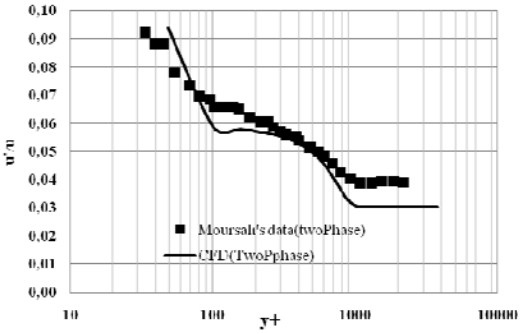

Fig. 10. Turbulent intensity profiles in vertical bubbly boundary layer. Comparison of the numerical results with the experimental data of Moursali *et al.* (1995)-(u=1m/s void fraction=0,015).

The predetermination of the turbulence is in good agreement with the measurement points. It should be noted also that the results show that in low velocity gradient zone and outside the boundary layer, we observe correctly an significant improvement of the turbulent intensity in the bubbly flows.

5. CONCLUSIONS

Diverse experimental works are studied the boundary layer development on a vertical flat plat. The results show the logarithmic behaviour for the near wall average velocity profiles in two phase flows. These data also prove that the constants of the logarithmic contours are sensibly modified in bubbly flows and depend on the amplitude of the wall void fraction peaking. A new law of wall was proposed where mixing velocity scale is a function of local parameters for two-phase flows. The present wall law was compared against experimental data using a CFD code. A good concordance between the profiles from the logarithmic phase flow model and the experiments was achieved.

REFERENCES

Antal, S. P., R. T. Lahey and J. E. Flaherty (1991). of Phase distribution in Fully Developed Laminar Bubbly Two-phase Flow, *International Journal of Multiphae Flow* 17, 635-652.

Drew, D. and R. T. Lahey (1982). Phase Distribution Mechanisms in Turbulent Two-Phase Flow in a Circular Pipe, *Journal of Fluid Mechanics* 117, 91-106.

Favre, L. (2006). A Rigorous Framework for Model-Driven Development, Advanced Topics in *Database Research*, vol. 5 edited by Keng Siau © 2006, Idea Group Inc.

Frank, T., P. J. Zwart, E. Krepper, H. M. Prasser, and D. Lucas (2008). Validation of CFD models for mono-and polydisperse air-water two-phase flows in pipes, *Nuclear Engineering and Design* 238(3), 647-659

Ishii, M. and N. Zuber (1979). Drag Coefficient and Relative Velocity in Bubbly, Droplet or Particulate Flows, *AIChE*, 25, 843-855.

Kuo, J. T. and G. B. Wallis (1988). Flow of bubbles through nozzles, *Int. J. Multiphase Flow* 14 (5), 547.

Lamb, H. (1932). hydrodynamics, *sixth ed Cambridge University Press New York*, 1932.

Lance, M. and J. Bataille (1991). Turbulence in the liquid phase of a uniform bubbly air water flow, J. Fluid Mech. 222, 95-118.

Llegendre, D. and J. Magnaudet (1998). The lift force on a spherical bubble in a viscous linear shear flow*, Journal of Fluid Mechanics*, 368, 81–126.

Lopez, B. M., S. J. Lee, R. T. Lahey and O. C. Jones (1994). Development of a k-epsilon model for bubbly two-phase flow. *Journal of Fluids Engineering* 116, 128-134.

Lopez, M. B., R. T. LaheyJr and O. C. Jones (1994). Phase Distribution in Bubbly Two-Phase Flow in Vertical Ducts, *International Journal of Multiphase Flow* 20, 805-818.

Maher, D., B. Ghazi, and C. Jamel (2013). A Two Time Scales Turbulence Model of Turbulent Bubbly Flows International Journal of Fluid Mechanics Research.v40.i3. 10, 185-203

Marie, J., E. Moursali and S. Tang Cong (1997) Similarity law and turbulence intensity profiles in a bubbly boundary layer at low void fraction"International journal of multiphase flow 23(2), 227-247.

Mikielewicz, D. (2003). Hydrodynamics and heat transfer in bubbly flow in the turbulent boundary layer .International journal of heat and mass transfer 46(2), 207-220.

Moursali, E., J. L. Marié and J. Bataille (1995). An upward turbulent bubbly layer along a vertical flat plate, Int. J. of Multiphase flow. 21(1), 107-117.

Murakawa, H., H. Kikura and M. Aritomi (2003). Measurement of Liquid Turbulent Structure in Bubbly Flow at Low Void Fraction Using Ultrasonic Doppler Method", Journal of Nuclear Science and Technology, 40(9), 644-654.

Ramstorfer. F., H. Steiner and G. Brenn (2008). Modeling of the microconvective contribution to wall heat transfer in subcooled boiling flow *International Journal of Heat and Mass Transfer. 51*(15-16), 4069-4082.

Troshko, A. (2000). *A two equation multidimentional model of turbulent bubbly flows* (Ph.D. thesis), the Texas A&M University, USA.

Saffman, P. G. (1968) .The lift on a small sphere in a slow shear flow, *J. Fluid Mech*. 31, 624.

Santarelli, C., J. Roussel and J. Fröhlich (2016). Budget analysis of the turbulen tkinetic energy for bubbly flow in a vertical channel, *Chemical EngineeringScience* 141(2016)46–62.

Sato, Y., M. Sadatomi and K. Sekoguchi (1981). Momentum and heat Transfer in Two-phase Bubble Flow, *Int. J. Multiphase Flow* 7, 179-190.

Schiller, L. and A. Naumann (1933). Uber die grundlegenden Berechnungen bei der Schwekraftaubereitung. *Zeitschrift des Vereines Deutscher Ingenieure* 77(12), 318-320.

Tomiyama, A. (1998). Struggle with Computational Bubble Dynamics, *Multiphase Science and Technology* 10, 369-405.

Troshko, A. and Y. A. Hassen (2001). A two-equation turbulence model of turbulent bubbly flows, *Int. J. Mult. Flow* 27, 1965-2000.

Vaidheeswaran, A., D. Prabhudharwadkar, P. Guilbert, R. John, J. Buchanan and M. L. Bertodano (2016). New Two-Fluid Model Near-Wall Averaging and Consistent Matching for Turbulent Bubbly Flows, ASME Journal of Fluids Engineering.

Wilcox, D. C. (1993). Turbulence Modeling for CFD, *DCWIndustries*, La Canada, CA, 104-110.

Xiaoping, G., Z. Li, L. Wang, X. Li and Y. Cheng (2015) A dual-scale turbulence model for gas-liquid bubbly flows, *CJCHE* 392

Yassin, A. H. (2014). Full-field measurements of turbulent bubbly flow using innovative experimental techniques. Texas A & M University. CASL-8-2014-0209-000.